Andrew C. Tam
Richard D. Balanson

Lasers in Electrophotography

We review the recent advances in the use of laser sources in the field of electrophotography. New experimental investigations of the photogeneration and transport processes utilized in electrophotography are now possible because of the short pulse duration, high peak power, high collimation, monochromaticity, and/or coherence of a laser source. Also, the increasing availability of reliable and inexpensive lasers has resulted in many new technological uses of lasers in electrophotographic applications. In addition to the continued use of HeNe and HeCd lasers, new products have been configured with GaAs lasers.

Introduction

Electrophotography [1], the photoelectric formation of latent electrostatic images and the development of these images, is an old technique invented by Carlson in 1938. The application of electrophotography is widespread; however, the various physical or chemical phenomena involved in electrophotography are frequently poorly understood, and many applications of electrophotography remain empirical. The difficulties in scientific investigations in electrophotography include the following: 1) The subject is multidisciplinary, involving quantum physics, classical physics, surface science, chemistry, crystallography, statistics, etc. 2) Ultrafast phenomena (*e.g.*, with time scales on the order of picoseconds) are involved, for example, in some photocarrier generation and relaxation processes. For these studies, very fast excitation and detection schemes are needed. 3) Ultraslow phenomena (*e.g.*, with time scales on the order of days or months) are also involved, for example, in some effects associated with carrier trapping and detrapping processes. For these studies, reproducibility and history-dependent effects are troublesome.

The advance of laser sources in recent years has provided new tools for understanding the effects involved in electrophotography. Also, the increasing availability and reliability of various lasers in the past ten years have opened up many new possible technological applications of lasers in electrophotography. The aim of the present review is to provide a survey of the usefulness of lasers in this field. We present examples of both how laser sources are exploited to provide further scientific understanding of the origins of electrophotography (photocarrier generation and transport in semiconductors) and new applications of lasers in electrophotographic technologies. This review is not meant to be exhaustive, but rather to provide an insight into one of the many useful roles that lasers have played in modern science and technology.

Lasers for studying electrophotographic materials

In the process of electrophotography (EP), an optical image is projected onto a photoreceptor situated in an applied electric field. The photoreceptor is composed of materials that generate carriers by optical absorption (photoconductor) and materials that subsequently allow these carriers to be transported under the influence of the applied field. Desirable characteristics of the photoreceptor are high photocarrier generation efficiency, broad spectral response, fast carrier transport with low carrier trapping probability, and low dark conductivity. Over the past ten years, lasers have been used to probe the generation and transport properties of photoreceptors. The advantages of using laser sources in these studies are that they are easily modulated or pulsed, highly collimated and focusable, and monochromatic. As yet, little advantage has been taken of the coherence of the laser beam, although interference and nonlinear beam-mixing techniques should prove useful for studying the photoconduction properties of some of the EP materials. We restrict our discussions in this article to the use of lasers to study EP materials that are usually thin layers of amorphous semiconductors (*e.g.*, Se, As_2Se_3, a-Si, organic semiconductors) or finely powdered semiconductors (*e.g.*, CdS, CdSe, ZnO, organic semiconductors). The broad field of laser studies of semiconductors in general is not covered in this article, nor is the general field of laser-induced photoconductivity. Representative examples are described that show how laser sources can be profitably used to study carrier generation and transport properties of materials useful in EP applications. We discuss studies first on charge generation and then on charge transport.

• *Dynamics of photocarrier generation*

Despite extensive work on the photocarrier generation mechanisms in amorphous semiconductors and organic materials [2, 3], little is known of the exact dynamics of the carrier generation. The phenomenological model generally used to explain the photocarrier generation is the *Onsager model* [4, 5]. In this model, the optical absorption in the amorphous semiconductor can produce a geminate electron-hole (e-h) pair with probability ϕ_0. The e-h pair can then either undergo geminate recombination or dissociation by diffusive motion under the influence of an external electric field, the latter with probability f. The photocarrier generation efficiency is the product of probabilities $\phi_0 f$. This Onsager model has apparently satisfactorily explained the photocarrier generation efficiencies (depending on the applied field) of amorphous semiconductors like polyvinyl carbazole (PVK) and its complexes [4], Se [5], triphenylamine-doped polycarbonate [6], and others. However, the detailed dynamics of the photocarrier generation process remains unknown. For example, the time developments of the formation of the e-h pair from the optically excited molecule and the Onsager dissociation have not been studied.

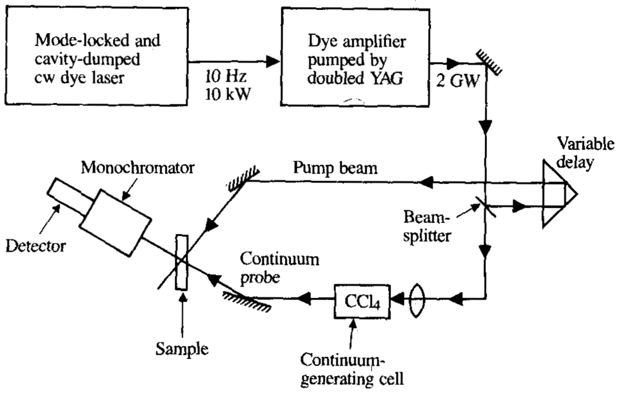

Figure 1 Experimental arrangement for picosecond continuum spectroscopy of amorphous and crystalline semiconductors (after Fork *et al.* [7]).

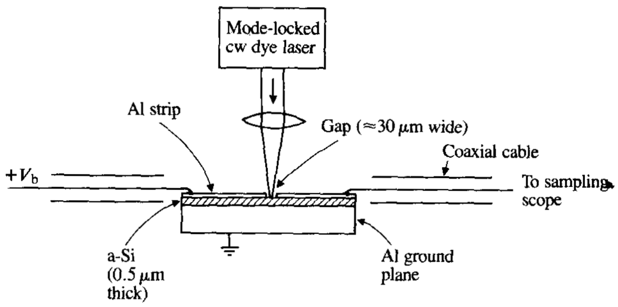

Figure 2 Microstrip transmission line geometry to measure fast transient photoconductivity of thin a-Si layer. The active area is a small gap between the thin aluminum microstrip (after Auston *et al.* [8, 9]).

The availability of short-pulse laser systems has now provided new possibilities for examining the dynamics of photocarrier generation. For example, Fork and coworkers [7] have demonstrated the usefulness of picosecond laser systems and picosecond laser-produced continuum sources to study the transient absorption features due to photocarriers produced in amorphous semiconductors (Fig. 1). The mode-locked and cavity-dumped cw dye laser they used produces narrow-band light pulses of 0.5-ps duration. A pulse is first amplified to 2-GW intensity by passing it through a dye amplifier and then beam-split: one beam (pump beam) is used to produce photocarriers in the sample (As_2S_3) and the other beam is focused into a liquid cell (*e.g.*, CCl_4) to produce a picosecond continuum source (probe beam). The probe is used to study the time-resolved absorption features in the sample due to the production of photocarriers. These authors observed a broad transient absorption band due to the photocarriers which extended from the visible to the infrared (beyond 1.6 μm). The time-development of this induced transient absorption showed a peak coincident with the pump pulse and a subsequent decay consisting of two components: a fast component decaying with a time constant of ≈ 3 ps and a slow one decaying with a time constant of $\gtrsim 300$ ps. More detailed studies of such induced absorption by photocarriers with higher time resolution should shed light on the dynamics of photocarrier generation in amorphous systems.

Another example of the use of picosecond light pulses to generate photocarriers in amorphous materials is the work of Auston and coworkers [8]. Here, fast transient photoconductivity was measured directly (Fig. 2). The sample was a thin amorphous silicon (a-Si) film which was low in hydrogen content. Such an amorphous material is characterized by fast relaxation times for the photoexcited carriers. The study was done with fast light pulses from a cw dye laser that was synchronously pumped by a mode-locked Ar^+ laser. The duration of the dye laser pulses was estimated as 8 ps. The transient photoconduction current observed had a rise time of 25 ps and a full width at half maximum of 40 ps. Auston *et al.* [8] estimated from these data that the carrier relaxation times in a-Si of low hydrogen content (<0.5%) were $\lesssim$30 ps, and these short relaxation times represent rapid relaxation of "hot" photoexcited carriers from mobile extended states to immobile localized states. Indeed, their later work [9] revealed that a-Si films with higher defect densities (formed from e-beam sputtering of Si in the presence of oxygen) had carrier relaxation times that were even shorter, typically <10 ps. The finding of very fast photocarrier relaxations in a-Si with high defect densities (10^{19} spins/cm^3 or larger) is interesting. This is because the relaxation times in the highly hydrogenated form [10] of a-Si ($\approx$20% hydrogen) are much longer, typically many μs.

The picosecond laser studies of amorphous photoconductors just described indicates that photocarrier generation and thermalization processes are quite fast, and time scales on the order of picoseconds generally can be expected. This is also found for certain cases of crystalline organic photoconductors. For example, Schein *et al.* [11] have used third harmonic outputs from a Nd:glass laser with a pulsewidth of 8-ps duration to study transient photoconductivity in single-crystal anthracene. Their measurements indicate that the processes of photogeneration, polaron formation, and hot carrier motion are over within 800 ps of the light illumination, and they estimated that geminate pair formation was accomplished in <20 ps. Thus, we conclude that picosecond laser methods have provided some understanding of the photocarrier generation dynamics in low-mobility photoconductors; however, more precise experiments with better time resolutions are still needed to provide a more quantitative understanding.

The picosecond laser technique (*e.g.*, the pump-probe [7] and transient-photocurrent techniques [8]) just discussed are time-resolved ways of studying the time-development of photocarriers. However, these time-resolved methods are not the only ways to study the fast photocarrier dynamics; space-resolved methods should also be possible. For example, the coherent nature of laser light can be exploited. Two coherent laser beams can produce a *grating* of photocarriers in the photoconductor, and a third coherent laser beam can be scattered from this grating, giving a detectable signal beam. Such types of four-wave mixing methods [12–15] using cw or pulsed laser beams should provide valuable information on the spatial and temporal developments of photoexcited carriers in photoconductors.

- *Photocarrier recombination*

Photocarrier decay processes in amorphous photoconductors can be first-order processes (like trapping at impurity centers, dangling bonds, and at vacancies, etc.) or second-order processes (like bulk recombination). The use of pulsed laser beams provides high enough photon intensities so that second-order processes can be readily observed. Hughes [16] has taken advantage of this technique to perform the first measurements of bulk recombination processes in a thin film of PVK/TNF (poly-N-vinylcarbazole/trinitrofluorenone) using a pulsed Q-switched ruby laser. Hughes discovered that bulk recombination processes of photocarriers in amorphous materials can be described by a Langevin recombination model [17] that is usually used to explain recombination in dense gaseous plasmas.

The Langevin recombination model is basically a random-walk or diffusive type of recombination motion between a positive and a negative charge. It holds when the mean free path is much shorter than the average separation between charges. In this case, the rate of approach between the positive and negative charges is given by

$$\frac{ds}{dt} = -\mu \frac{e}{\varepsilon s^2}, \tag{1}$$

where s is the instantaneous charge separation, μ is the sum of mobilities (of the positive and negative charges), and ε is the dielectric constant. By integrating Eq. (1) from s_0 to 0, where s_0 is the initial ion separation, we obtain the recombination time τ_{rec} as

$$\tau_{rec} = \frac{s_0^3 \varepsilon}{3\mu e}. \tag{2}$$

By equating charge density N with $1/(4\pi s_0^3/3)$, we obtain

$$\tau_{rec} = \frac{\varepsilon}{4N\pi\mu e}. \tag{3}$$

This is the Langevin recombination formula, which states that the bulk recombination rate is proportional to the combined mobility and to the square of the carrier density because

$$\frac{dN}{dt} = \frac{N}{\tau_{rec}} = 4N^2\pi\mu e/\varepsilon.$$

Hughes [16] used a pulsed ruby laser beam to produce transient carriers in the amorphous photoconductor, with initial carrier concentration n_0 in the range of 10^{11} to 3×10^{15} cm^{-3}. He showed that the actual number n of carriers collected is smaller than n_0, and that n/n_0 decreases monotonically as n_0 increases. His data are consistent with the Langevin bulk recombination model, showing that bulk recombination is quite significant in amorphous organic semiconductors like PVK/TNF when carrier concentrations exceed 10^{14} cm^{-3}. More recently, Mey *et al.* [18] have examined bimolecular recombination in xerographic photoconductors (of the aggregate organic type) using a pulsed dye laser. Such bimolecular recombinations contribute to a high-intensity reciprocity failure. Their experimental results again indicate that the Langevin-type recombination becomes significant at exposures exceeding 10^{12} photons/cm^2.

- *Photoacoustic studies of photoconductivity*

Photoacoustic methods [19] have recently been established as useful tools to probe the properties of condensed matter; *e.g.*, very weak absorption spectra can be measured [20]. The acoustic waves are generated by thermal decay in the medium after optical excitation. Suppose that in a photoconducting material only two competing channels are possible after optical excitation: photocarrier production and thermal decay. Then, any changes in the photocarrier production efficiency (*e.g.*, due to changes in an applied electric field or external load resistor) will be accompanied by related changes in the thermal decay probability and photoacoustic signal intensity.

Cahen [21] first demonstrated the complementary nature of photoelectricity and photoacoustics by studying the variation in the photoacoustic signal from a solar cell when the external load resistance is changed. He found that the photoacoustic signal intensity decreases as the photoelectric power output increases, and that the photoacoustic signal is minimized when the external load resistance equals the internal resistance of the solar cell.

Tam [22] has extended Cahen's idea by using the laser photoacoustic technique to examine photocarrier generation efficiencies of organic dye photoconductors of importance in EP applications. The photoconductor studied is a layered structure [23] composed of a dye film of thickness $\lesssim 1$ μm on aluminized Mylar, covered by a suitably doped polycarbonate film of thickness ≈ 20 μm. Photocarriers are generated in the dye film (*charge-generation layer*) and the applied electric field allows only holes to be injected into the doped polycarbonate film (*charge-transport layer*). The photocarrier generation efficiency Q (defined as the average number of mobile electrons or holes generated per photon absorbed) in this type of layered organic photoconductor is known [23] to be quite dependent on the electric field E, and is almost zero when E is zero. The value of Q at various applied fields has been measured using the photoacoustic apparatus described in Fig. 3. A krypton ion laser beam is modulated by an acousto-optic modulator at about 40 kHz frequency; the frequency is chosen to be at the fundamental mechanical resonance frequency of the piezoelectric transducer and sample assembly. The thermal diffusion length (which equals the square root of the thermal diffusivity/π times the chopping frequency) is about 1 μm at a 40-kHz frequency,

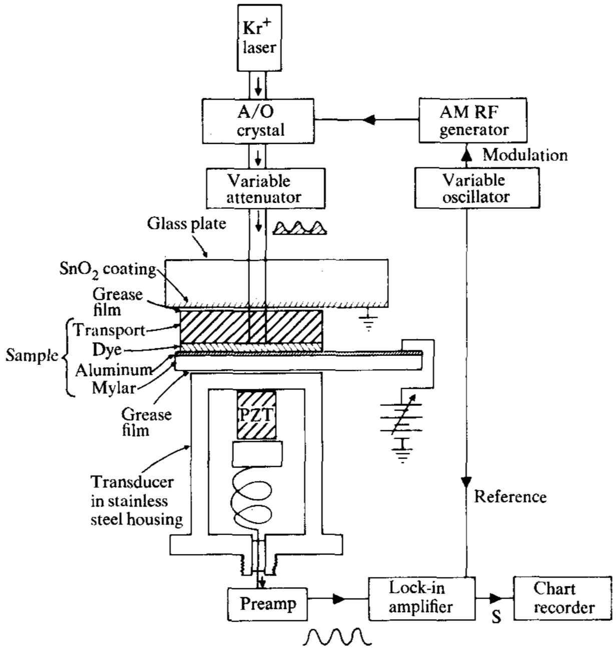

Figure 3 Schematics of the experimental arrangement to measure photoconductive properties of dye films at various applied electric fields. The sample thickness is not drawn to scale; the thicknesses of the transport, dye, aluminum, and Mylar layers are 20, 1, 0.1, and 75 μm, respectively. A spring-clamp to compress the transducer, sample, and conductive glass electrode together is not shown.

and hence the photoacoustic signal originates mainly from the dye layer. Otherwise, trapping would contribute to the heat, complicating the theory. The sample is compressed between a transparent electrode of SnO_2-coated glass and a lead zirconate titanate transducer, which has been described previously [20]. The photoacoustic signal S, detected by a lock-in amplifier, is found to depend on E. The thermal decay branch competes with the photocarrier generation branch when $E \neq 0$, but the thermal decay branch is the sole branch for $E = 0$. We may thus write

$$S(0) = KI_0; \tag{4}$$

$$S(E) = K[1 - Q(E)]I_0, \tag{5}$$

where K is a constant for the detection sensitivity, I_0 is the amplitude of the modulated light, and $Q(E)$ is the field-dependent quantum efficiency for the photocarrier generation. Hence,

$$Q(E) = [S(0) - S(V)]/S(0). \tag{6}$$

By this method, Tam [22] has been able to measure $Q(E)$ at low fields ($E \lesssim 2 \times 10^5$ V/cm), where severe trapping of photocarriers makes normal direct measurement (*i.e.*, by measuring the number of photocarriers collected at the electrodes) difficult.

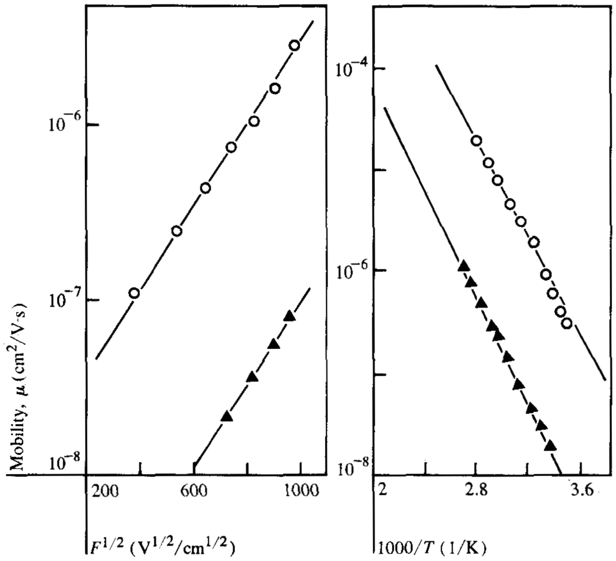

Figure 4 (a) Field dependence of hole- (○) and electron-drift (▲) mobilities at 24° and a PVK:TNF molar ratio of 1:0.2. (b) Temperature dependence of the mobilities at $E = 5 \times 10^5$ V/cm for the same molar ratio. (After Gill, Ref. [24(a)].)

• *Charge transport—transient photoconductivity*

Several authors have taken advantage of the high peak intensity and short pulse duration of a pulsed laser source to study transport properties in amorphous photoconductors. Typically, an optical pulse produces transient photocarriers in a well-defined space and time, and carriers of one sign are made to transport through the sample. Although the photogeneration process itself is very fast (on the order of ps), the transport process is generally much slower (for example, it generally takes many microseconds to move through a sample of thickness of $\approx$10 μm). Thus, light pulses of approximately nanosecond duration are adequate for transport property measurements, in contrast to the picosecond light pulses needed to investigate photogeneration processes.

Gill [24(a)] made some of the first investigations of transport properties in PVK/TNF complexes using a pulsed ruby laser as the light source. The light pulse was produced by a laser-induced breakdown spark (instead of directly from the laser), providing a nearly "white" source. This made it possible to use a filter to select a suitable spectral component for excitation of the sample; that chosen by Gill was in the ultraviolet, so that photocarriers were generated only in a thin surface layer of the sample. A voltage step was applied across the sample 1 ms before the light pulse to minimize field distortion due to dielectric relaxation, and the transient photocurrent was recorded on a scope. The sign of the voltage pulse determined whether electron or hole transport was being measured. The transit time τ_T was determined from the current transient observed, and the mobility μ was derived from

$$\mu = L^2/(\tau_T V), \tag{7}$$

where L is the sample thickness and V is the applied voltage.

Gill's results [24(a)] for the electron and hole mobilities, depending on the applied field E and the absolute temperature T, for a PVK:TNF complex are shown in Fig. 4. Remarkably, the results can be fitted by an empirical formula; both for electron and hole mobilities,

$$\mu = \mu_0 \exp -(W - \beta E^{1/2})/k_B T_{\text{eff}}\,; \tag{8}$$

$$1/T_{\text{eff}} = 1/T - 1/T_0\,. \tag{9}$$

Here, μ_0 and T_0 are constants depending only on the film composition, β and W are constants independent of composition, and k_B is the Boltzmann constant. Although Eq. (8) can be expected in terms of a Poole-Frenkel mechanism for trap-controlled mobility, it seems unrealistic [24] to assume the existence of large numbers of charged trapping centers of both polarities, as required in the Poole-Frenkel model. Furthermore, Eq. (8) does not fit the dependence of μ on E and T for other amorphous organic systems such as triphenylamine-doped polycarbonate [2]. Thus, the successful fit of Eq. (8) for the mobilities in PVK/TNF remains to be explained. However, the fact [24] that μ depends exponentially on the average separation between dopant molecules, but is relatively independent of the background matrix, suggests that conductivity in doped polycarbonate (for example) is due to hopping of carriers between dopant molecules.

Mobility is a complicated quantity in amorphous photoconductors. Besides the dependence on E and T just mentioned, it also may depend on doping, sample history, etc. Also, mobility is usually due to a dispersive transport [2] in amorphous materials, in contrast to nondispersive transport in crystalline materials. In other words, severe spreading in the carrier transit times exists, and no completely satisfactory transit time can be defined. A recent investigation of the dispersive transport in hydrogenated amorphous silicon using pulsed dye lasers has been reported by Hvam and Brodsky [24(b)]. A further complexity is that mobility can be time-dependent [25]. Orenstein and Kastner [26] have recently made an interesting study concerning the time-dependent mobility in As_2Se_3. They used a pulsed dye laser of 10-ns duration to produce transient photocarriers in amorphous As_2Se_3, and an ir probe beam to simultaneously measure the time development of photoinduced absorption and photoconductivity. The time dependence of the hole mobility is obtained by the following equations for the photocurrent i_p and the fractional changer in transmission ΔI for an incident probe intensity I:

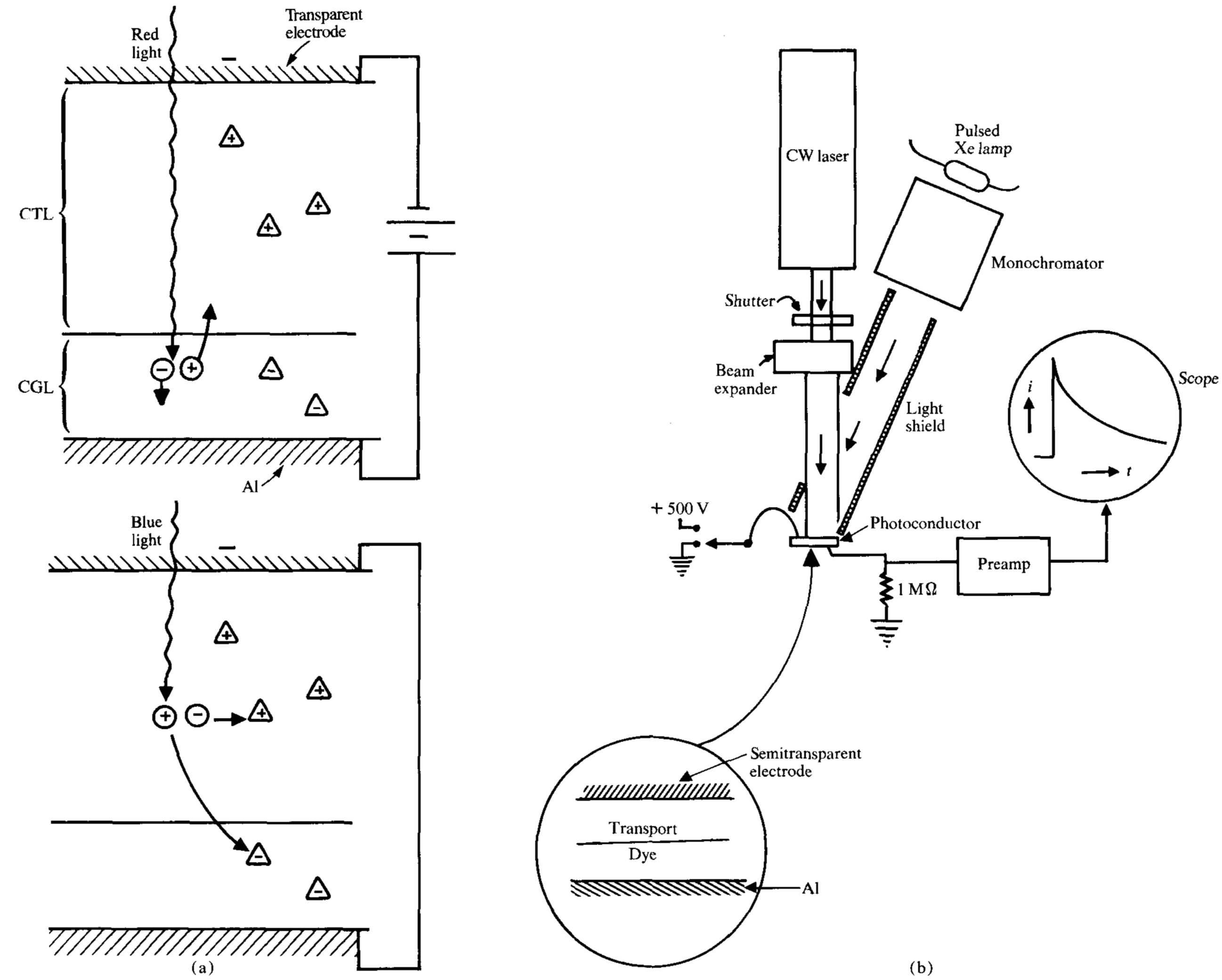

Figure 5 (a) Schematics to show the idea of production of trapped charges by red light (red-fatigue) in a layered photoconductor and for the removal of trapped charges by blue light (blue-revival). Transparent top electrodes with Al bottom electrodes. CTL and CGL stand for charge-transport layer and charge-generation layer. (b) Apparatus to study the production and removal by light of fatigue effects in photoconductors.

$$i_p = N_p we\mu E, \tag{10}$$

$$\Delta I/I = N_\alpha \sigma, \tag{11}$$

where N_p and N_α are the areal densities of charge carriers giving rise to the photocurrent and absorption, respectively, w is the width of the excited region, e is the electronic charge, E is the applied electric field, μ is the average mobility, and σ is the optical absorption cross section of the photocarriers. Eqs. (10) and (11) give

$$\mu(t) = \frac{i_p I}{\Delta I} \frac{N_\alpha(t)}{N_p(t)} \frac{\sigma}{weE}, \tag{12}$$

where t is time. Now, by assuming $N_\alpha(t) = N_p(t)$, Orenstein and Kastner [26] obtained a time-dependent mobility which was the same as that obtained by Pfister and Scher [25], who used a sandwich-cell configuration to observe the transient photocurrent due to the motion of the carriers in the absence of bulk recombination. The agreement of the two determinations of $\mu(t)$ indicates that the assumption $N_\alpha(t) = N_p(t)$ is correct. This is the first demonstration that the same photoexcited carriers are responsible for the phenomena of photoinduced absorption and photoconductivity.

• *Charge trapping and detrapping*

It has long been recognized that amorphous conductors with low mobilities are characterized by frequent trapping events. Roughly speaking, there are two types of trapping events. When the trapping energy is on the order of the thermal energy or smaller, the trapped carriers can subsequently be

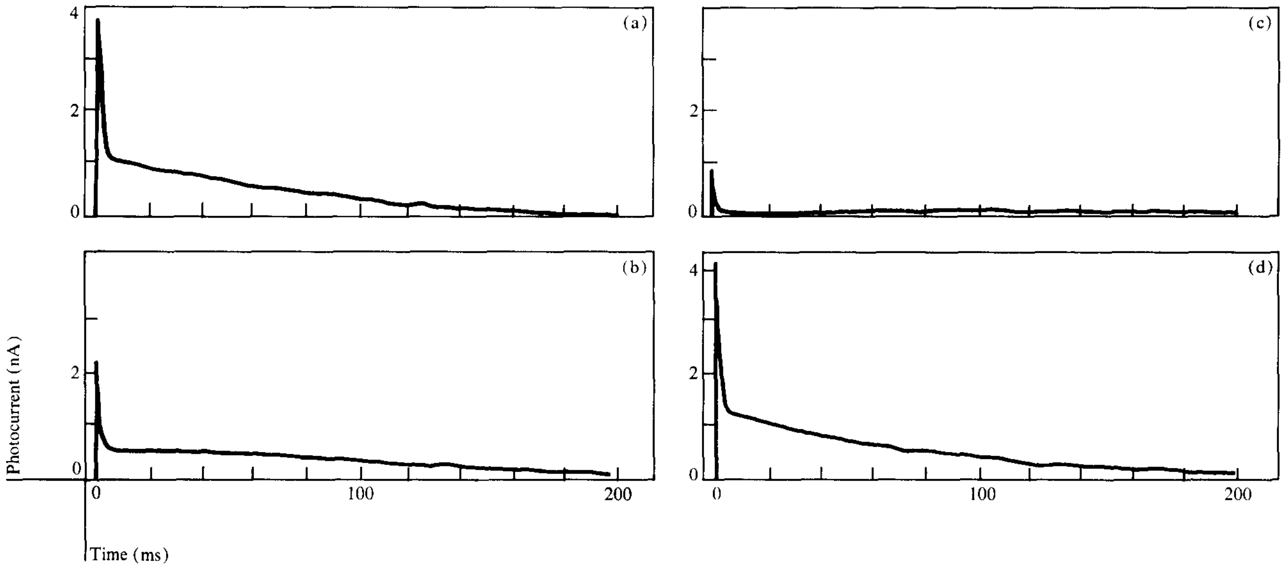

Figure 6 Observed transient photoconduction signals for methyl squarylium. The applied field is 2.3×10^5 V/cm; the probing pulse is $\approx 10^{-10}$ J at 830 nm of duration 0.1 ms at time = 0. (a) Initial fully sensitive photoconductor; (b) After an exposure to 647-nm light of energy density 0.5 mJ/cm^2 with field on; (c) After further exposure to 647-nm light of energy density 11 mJ/cm^2 with field on; (d) After exposure to blue light (400–550 nm) of energy density about 50 mJ/cm^2 with field off.

released by thermal excitation. This type of trapping and detrapping is the origin of trap-controlled mobility, which has been characterized by an activation energy in Arrhenius plots of mobility [2]. When the trapping energy is much larger than the thermal energy, the trapped charges take a long time to be released and they cause the occurrence of persistent internal polarization (PIP) [27, 28]. Persistent internal polarization in photoconductors frequently takes a long time (hours, days, or longer) to decay in the dark.

In the layered organic photoconductors [22] just mentioned, persistent internal polarization due to deeply trapped holes in the charge-transport layer is particularly hard to relieve. This is because the charge-transport layer only conducts holes, and electrons cannot be injected into it; hence, bulk recombination cannot occur. In efforts to quickly relieve the persistent internal polarization in layered photoconductors without resorting to thermal means (*i.e,* high temperature), Tam *et al.* [29, 30] have used various lines from a Kr^+ laser to examine whether photoexcitation of the dopant molecules in the transport layer may result in a decay of the trapped charges. The idea is shown schematically in Fig. 5(a). In the normal operation of the photoconductor in an electrophotographic application, the photoconductor is exposed to only red light, which is strongly absorbed by the charge-generation layer but not by the charge-transport layer. Thus, trapped positive charges in the charge-transport layer slowly build up due to injected holes. This is called the *red-fatigue* effect. In theory, irradiation of the layered photoconductor with blue or violet light, which is absorbed by the dopant molecules in the transport layer, produces photoconductivity in the transport layer itself, thus providing a possible means for the trapped holes to be conducted away. This effect is called the *blue-revival effect.*

The experimental apparatus [29] for testing these effects is shown in Fig. 5(b). Here, two light sources are used: a weak pulsed light source of duration 0.1 ms (obtained from a small pulsed Xe lamp and a monochromator) and a strong cw monochromatic light source (Kr^+ laser with output lines covering the visible range and near-uv and ir). The weak light source is used to probe the photocarrier injection efficiency (the number of charges collected per absorbed photon), and is weak enough ($<10^{-10}$ J/cm^2) so that it does not produce any fatigue or revival effects. The strong light source, in conjunction with a shutter and a suitable attenuator, is used to precondition the photoconductor sample. Experimentally, the photoinjection efficiency of a freshly prepared, dark-adapted photoconductor is first measured by using the pulsed light only. The photoconductor is then exposed to a known amount of light energy (typically 1 mJ/cm^2) from the cw source at a given wavelength. With the cw light source off, the photoinjection efficiency is probed again by using the weak pulsed light. This "exposure-probe" procedure is repeated for various amounts of exposure to the cw light source at various wavelengths.

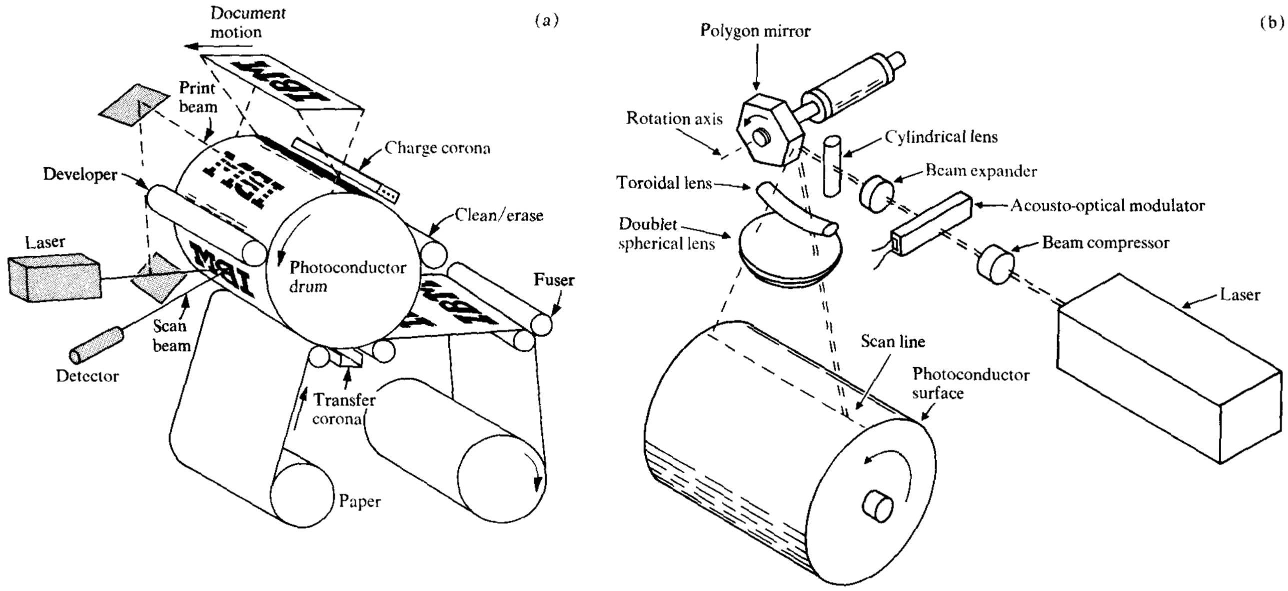

Figure 7 (a) Electrophotographic copying process. The grey-toned boxes show a possible configuration of an electrophotographic printer/scanner using a raster scanning laser beam. (b) The use of a laser to scan a photoconductive drum and thus use electrophotography for printing.

Some experimental results obtained by Tam and coworkers [29] are shown in Fig. 6. Here, we see that the concepts of red fatigue and blue revival for some types of photoconductors of interest in electrophotography are verified. For example, we see that exposure to 11 mJ/cm^2 of red light (647 nm) totally fatigues the photoconductor (*i.e.*, the photoinjection efficiency has drastically decreased from the original value), while subsequent exposure to 50 mJ/cm^2 of blue light (482 nm) causes a substantial recovery of the photoinjection efficiency.

We have also performed tests [29] of these effects in an EP copier robot. Persistent internal polarization (PIP) due to trapped charges is usually undesirable in EP applications (although it may be useful in other applications [31]), and the robot work on layered organic photoconductors may indicate that PIP can be reduced by the blue-revival effect. Hence, we have performed measurements of the sensitivity and stability of the photoconductor in an EP machine robot using either a blue or red erase lamp. Unfortunately, the test results appear inconclusive; *i.e.*, depending on the test conditions, a blue erase lamp may cause less fatigue in the photoconductor than the red erase lamp, or vice versa at other test conditions. It appears that the blue-revival effect is not obvious in the EP machine robot configuration because the PIP induced by the copying process is always much smaller compared to the PIP in the previous experiment with sandwiched photoconductors. More work is needed to understand the effect of the erase lamp (spectrum and intensity) on the weak PIP induced in a photoconductor in actual EP machine operation.

Lasers in electrophotographic devices

In addition to their use in exploring basic physical phenomena of photoconductive materials, lasers have also been applied to actual printing processes in which the laser "writes" on a photoconductive substrate. It will be worthwhile to first describe the steps involved in using electrophotography to copy a document. As can be seen in Fig. 7(a), the heart of the electrophotographic copier is typically a photoreceptor drum which rotates past several stations in the machine [32]. This material can be either inorganic (*e.g.*, Se or CdS [33, 34]) or organic (*e.g.*, a diazo [35] or thiapyrilium dye [36]). The key material property is that it can be charged and will hold a high voltage (typically 800 V) in the dark, but when exposed to light it will decay to low voltage (typically 100 V). In a copier device, the cycle begins by uniformly charging the photoreceptor by passing it under a corona (in this example the charging is negative). The drum then rotates past the exposure station where white light reflecting off a printed document is imaged onto the photoreceptor. Wherever dark characters existed on the original printed page, no change occurs in the surface voltage; where white background existed, the photoconductor is illuminated and thus discharged. The result is that an electrostatic image of the document is produced on the photoconductive drum,

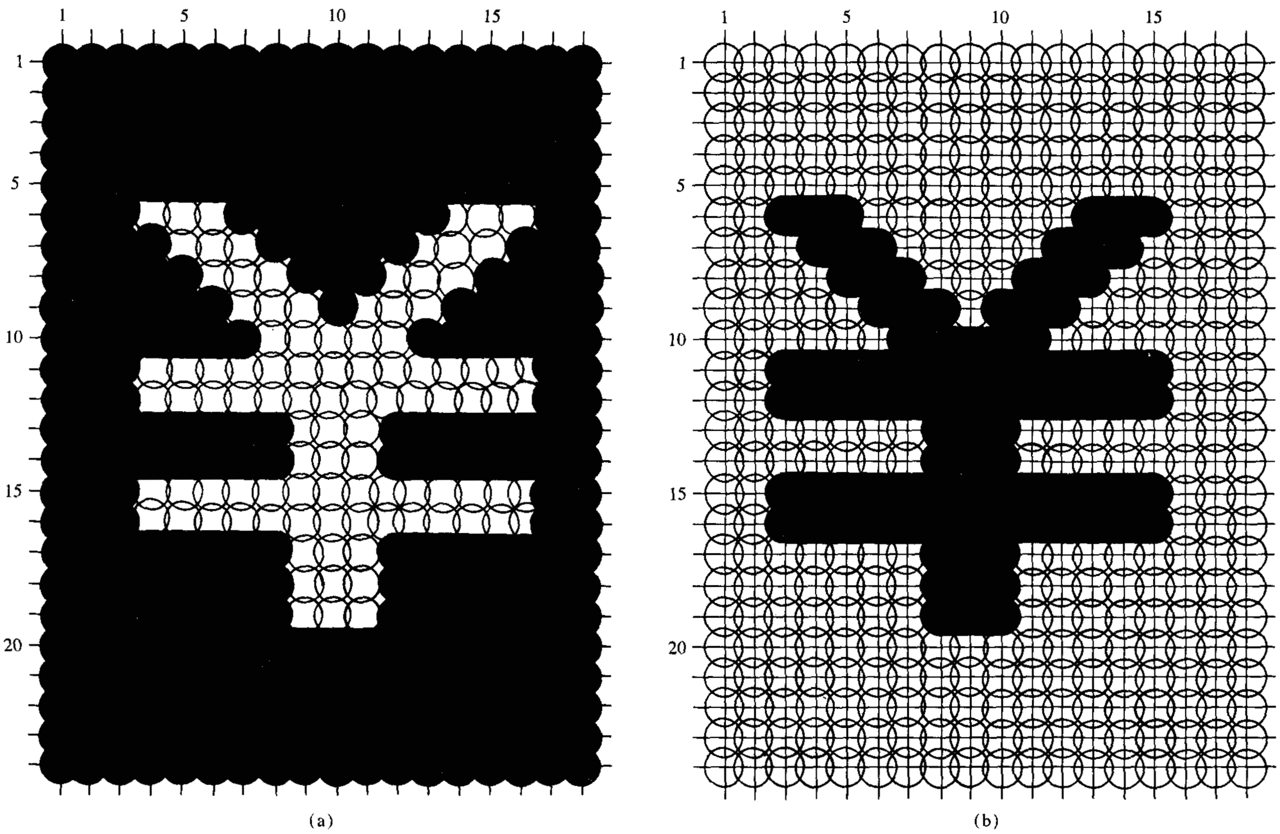

Figure 8 Scan patterns for process in which laser "writes" (a) the background and (b) the characters. Open circles represent "off" pulses and dark spots represent "on" pulses.

in which the initial characters or images are represented by areas of high charge and the white background of the original is represented by low or ideally zero charge.

The next step in the process is the visualization of the electrostatic image with ink. A typical material used is a thermoplastic resin filled with carbon black (toner). The toner is charged to the opposite sign from that of the photoconductor and is thus attracted to the areas of high opposite field (*i.e.*, the electrostatic image areas). At the end of this step in the cycle, the electrostatic image on the photoconductor has been converted into a visible toned image. Next, the toner is transferred from the photoconductor to paper by electrostatically charging the back side of the paper and attracting the oppositely charged toner to it. The copy is now complete except that the toner is not held permanently to the paper. To accomplish this, the paper is sent through a fusing station where it is heated and/or subjected to pressure to fuse the thermoplastic powder. Finally, the small amounts of residual toner left on the photoconductor are removed by a cleaning station and the cycle is complete. Copiers based on this technology have been commercialized with speeds ranging from 10 to over 100 copies per minute [37].

- *Laser printers*

The electrophotographic copying process is one in which light is used to effect an electrostatic charge decay in a photoconductive material. An obvious extension of this process is therefore to use a laser as a controlled source of light to "write" an image onto the photoconductor, thus replacing the light reflecting off a document [Fig. 7(b)].

There are two possible implementations of laser electrophotography. If one attempts to replace the exposure station [Fig. 7(a)] directly with a laser printhead, it is necessary to have the laser write the background of the desired document [38]. This arises since in copying processes the background of the original is the light area and the characters are unilluminated areas. In Fig. 8(a), if the round spots are used to represent the addressed positions of the laser scanning printhead to duplicate the copying process, the open circles would represent laser-*on* pulses and the dark spot laser-*off* pulses [39]. If this exposure is chosen, the remaining steps in the electrophotographic process remain unchanged. On the other hand, if one chooses to write the characters and not the background with the laser, the characters would be areas of low voltage, with a high-voltage background. Figure 8(b)

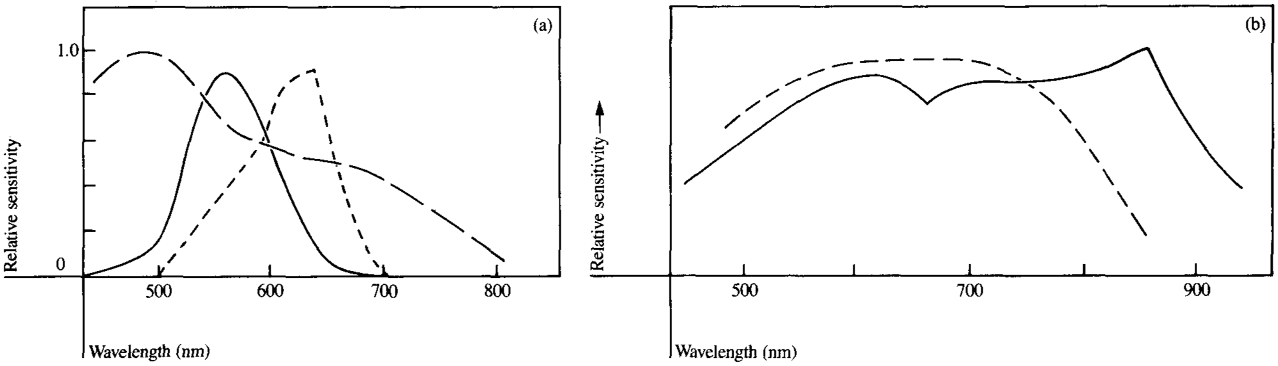

Figure 9 (a) Electrophotographic spectral sensitivity of commonly used photoconductors, Se-Te (—) and an IBM diazo dye (---), compared to the sensitivity of the eye (—). (b) Electrophotographic sensitivity of two ir-sensitive photoconductors. The squarylium photoconductor (—) is a layered organic system, and the CdS (—) is a specially prepared doped inorganic system.

would represent this case. To develop this image, it would be necessary to suitably bias the developer station so that the background appears at zero or low voltage and the exposed areas appear at a high positive voltage. This second "reversed-development" approach has by far been the most commonly employed in commercial printers. The IBM 3800 Printer uses this approach and produces 220 documents per minute [40]. In contrast, the IBM 6670 Printer [38] uses the standard-development process (laser writes background) and produces 37 documents per minute. In both cases the laser is scanned in a raster rather than a vector mode.

- *Types of laser*

Because photoconductors used in electrophotographic processes are typically quite sensitive (requiring from 0.5 to 2.0 $\mu J/cm^2$ to discharge an 800-V surface potential), the laser power necessary to produce high-speed electrophotographic printers is relatively small. Excluding losses due to the modulator and optics, the effective laser power necessary to produce a 200-copy-per-minute printer is 4 mW. In addition, since the photoconductors used in the EP process were originally chosen to copy documents and thus to match the spectral response of the eye [see Fig. 9(a)], inexpensive and reliable visible lasers were chosen for the EP printing process. For pure Se photoconductors, HeCd was the ideal choice; for more red-sensitive photoconductors such as PVK/TNF, thiapyrilium, and Se alloys, HeNe was chosen.

More recently, to reduce cost, size, and power usage, there has been a drive to move from gas lasers to solid state GaAs devices. Unfortunately, common commercial GaAs lasers typically produce 850-nm light, and conventional photoconductors show little or no sensitivity at this wavelength [Fig. 9(a)]. Two possible methods exist for adapting these devices. First, by doping the GaAs, it is possible to shift the wavelength toward the visible region, and experimental room-temperature devices have been produced which lase at 640 nm [41]. It is also possible to shift the spectral sensitivity of the photoconductor into the near-infrared portion of the spectrum by either doping [42] or formulating a system with dyes possessing either exclusive ir sensitivity [such as nickel bis(dithiolene) dyes] [43] or sensitivity across both the visible and near-infrared wavelengths (such as squarylium-layered photoconductors) [23] [see Fig. 9(b)].

- *Document scanners*

Since in order to produce an electrophotographic laser printer it is necessary to have a raster scanning laser beam, a logical extension of this printing technology is to produce a document scanner, a device which not only prints but also will digitize original documents (effectively a facsimile device). At least two configurations could be used to implement this idea.

First, the laser beam could scan the document directly [see Fig. 7(a)]. A simple mirror could be placed in front of the laser, deflecting the beam away from the photoconductor drum and up to the document. The light reflecting off the printed page could then be collected by a number of devices such as lenses, diodes, or light tubes. A limitation of this technology is the "color-blindness" of the laser beam. If for example one chooses to use a HeNe laser as the printing/scanning beam, all documents encoded by the device must have high reflectivity to red light in the background regions and must use an ink which absorbs red light; *i.e.*, the device is blind to red-reflecting ink. If one chooses to use a GaAs laser, the situation is worse. The document must be printed with ink absorbing in the near-infrared. With the exception of a few water-based inks (nigrosin and sulfur black) and carbon black dispersions, many commercial inks have little or no absorption beyond 750 nm [44]. Thus, the scanning function would be inadequate, missing information from many documents.

A second method of implementing the scanning laser would be to scan the toned photoconductor image instead of the document itself. This approach overcomes many of the problems just described. Since the typical photoconductor used in these processes is almost panochromatic in its response to light, virtually all information on the document would be seen by the photoconductor. Secondly, since toner contains carbon black, which has flat and high absorption across the visible and near-infrared spectrum, any laser could be used and no information would be lost due to color-blindness. The grey-toned boxes in Fig. 7(a) show a possible configuration for such a device.

Summary

We have seen that the advent of new laser sources (combined with novel techniques such as photoacoustic methods) over the past ten years has allowed a more thorough understanding of the basic photoconductive processes of charge generation and transport. In addition, the availability of inexpensive and reliable gas lasers, and more recently solid state lasers, combined with basic electrophotography, has provided new high-speed, nonimpact, all-points-addressable printing technology.

Acknowledgments

We thank W. D. Gill, B. Grant, and W. Imaino for useful comments on this manuscript.

References and notes

1. See for example R. M. Schaffert, "Electrophotography," Focal Press, London, 1965; J. H. Dessauer and H. E. Clark, "Xerography and Related Processes," Focal Press, London, 1965; V. M. Fridkin, "The Physics of the Electrophotographic Process," Focal Press, London, 1973.
2. J. Mort and G. Pfister, "Photoelectronic Properties of Disordered Solids: Molecularly-Doped Polymers," *Polymer Plastics Technol. Eng.* **12,** 89–139 (1979).
3. W. D. Gill, "Polymeric Photoconductors," Ch. 8 of *Photoconductivity and Related Phenomena,* J. Mort and D. M. Pai, Eds., Elsevier, New York, 1975, pp. 303–334.
4. P. J. Melz, "Photogeneration in Trinitrofluorenone-poly(N-vinylcarbazole)," *J. Chem. Phys.* **57,** 1694–1699 (1972).
5. D. M. Pai and R. C. Enck, "Onsager Mechanism of Photogeneration in Amorphous Selenium," *Phys. Rev. B* **11,** 5163–5174 (1975).
6. P. M. Borsenberger, W. Mey, and A. Clowdry, "Hole Transport in Binary Solid Solutions of Triphenylamine and Bisphenol-A-polycarbonate," *J. Apply. Phys.* **49,** 273–279 (1978).
7. R. L. Fork, C. V. Shank, A. M. Glass, A. Migus, M. A. Bosch, and J. Shah, "Picosecond Dynamics of Optically Induced Absorption in the Bandgap of As_2S_3," *Phys. Rev. Lett.* **43,** 394–398 (1979); "Picosecond Spectroscopy of Amorphous Semiconductors Using Nonlinear Techniques," *J. Noncryst. Solids* **35–36,** 963–968 (1980).
8. D. H. Auston, P. Lavalland, N. Sol, and D. Kaplan, "An Amorphous Silicon Photodetector for Picosecond Pulses," *Appl. Phys. Lett.* **36,** 66–68 (1980).
9. D. H. Auston, A. M. Johnson, P. R. Smith, and J. C. Bean, "Picosecond Optoelectronic Detection, Sampling, and Correlation Measurements in Amorphous Semiconductors," *Appl. Phys. Lett.* **37,** 371–373 (1980).
10. See *e.g.* H. Fritzche, "Characterization of Glow-Discharge Deposited a-Si: H," *Solar Energy Mater.* **3,** 447–501 (1980).
11. L. B. Schein, R. W. Anderson, R. C. Enck, and A. R. McGhie, "Subnanosecond Time-Resolved Transient Photoconductivity in Anthracene," *J. Chem. Phys.* **71,** 3189–3193 (1979).
12. D. M. Bloom and G. C. Bjorklund, "Conjugate Wave-front Generation and Image Reconstruction by Four-Wave Mixing," *Appl. Phys. Lett.* **31,** 592–594 (1977).
13. J. R. Salcedo, A. E. Siegman, D. D. Dlott, and M. D. Fayer, "Dynamics of Energy Transport in Molecular Crystals: The Picosecond Transient-Grating Method," *Phys. Rev. Lett.* **41,** 131–134 (1978).
14. D. S. Hamilton, D. Heiman, J. Feinberg, and R. W. Hellworth, "Spatial-Diffusion Measurements in Impurity-Doped Solids by Degenerate Four-Wave Mixing," *Opt. Lett.* **4,** 124–125 (1979).
15. M. D. Levenson, "High-Resolution Imaging by Wave-front Conjugation," *Opt. Lett.* **5,** 182–184 (1980).
16. R. C. Hughes, "Bulk Recombination of Charge Carriers in Polymer Films: Poly-N-vinylcarbazole Complexed with Trinitrofluorenone," *Appl. Phys. Lett.* **21,** 196–198 (1972).
17. M. P. Langevin, "Ionization des Gaz," *Ann. Chim. Phys.* **28,** 289–384 and "Recombinaison et Mobilités des Ions dans les Gaz," *Ann. Chim. Phys.* **28,** 433–530 (1903).
18. W. Mey, E. I. P. Walker, and D. C. Hoesterey, "Bimolecular Recombination in Aggregate Organic Photoconductors," *J. Appl. Phys.* **50,** 8090–8094 (1979).
19. See *e.g. Optoacoustic Spectroscopy and Detection,* Y. H. Pao, Ed., Academic Press, Inc., New York, 1977.
20. (a) A. C. Tam and C. K. N. Patel, "Optical Absorption of Light and Heavy Water by Laser Optoacoustic Spectroscopy," *Appl. Opt.* **18,** 3348–3357 (1979); (b) A. C. Tam and C. K. N. Patel, "High-Resolution Optoacoustic Spectroscopy of Rare-Earth Oxide Powders," *Appl. Phys. Lett.* **35,** 843–845 (1979).
21. D. Cahen, "Photoacoustic Determination of Photovoltaic Energy Conversion Efficiency," *Appl. Phys. Lett.* **33,** 810–811 (1978).
22. A. C. Tam, "Optoacoustic Determination of Photocarrier Generation Efficiencies of Dye Films," *Appl. Phys. Lett.* **37,** 978–981 (1980).
23. P. J. Melz, R. B. Champ, L. S. Chang, C. Chion, G. S. Keller, L. C. Liclican, R. R. Neiman, M. D. Shattuck, and W. J. Weiche, "Use of Pyrazoline-Based Carrier Transport Layers in Layered Photoconductor Systems for Electrography," *Photog. Sci. Eng.* **21,** 73–78 (1977).
24. (a) W. D. Gill, "Drift Mobilities in Amorphous Charge-Transfer Complexes of Trinitrofluorenone and Poly-N-vinylcarbazole," *J. Appl. Phys.* **43,** 5033–5040 (1972); (b) J. M. Hvam and M. H. Brodsky, "Dispersive Transport and Recombination Lifetimes in Phosphorous-Doped Hydrogenated Amorphous Si," *Phys. Rev. Lett.* **46,** 371–374 (1981).
25. G. Pfister and H. Scher, "Dispersive (Non-Gaussian) Transient Transport in Disordered Solids," *Adv. Phys.* **27,** 747–798 (1978).
26. J. Orenstein and M. Kastner, "Time-Resolved Optical Absorption and Mobility of Localized Charge Carriers in a-As_2Se_2," *Phys. Rev. Lett.* **43,** 161–165 (1979).
27. H. P. Kallman, J. Rennert, and M. Sidran, "A Photographic Process Using Persistent Internal Polarization in Phosphors," *Photog. Sci. Eng.* **4,** 345–353 (1960).
28. B. M. Golovin, I. S. Zheluev, N. T. Kashukeev, I. N. Orlov, V. M. Fridkin, L. Y. Mogilevskaya, and A. S. Antonov, "A New Electrophotographic Process Effected by Means of Combined Electret Layers," *Sov. Phys. Dokl.* **12,** 1351–1354 (1959).
29. A. C. Tam and R. Kerth, "Revival of Fatigued Layered Photoconductors by Light," IBM Research Division, 5600 Cottle Rd., San Jose, CA; unpublished report.
30. R. Balanson, W. D. Gill, and A. C. Tam, "Revival of Fatigued Photoconductors," *IBM Tech. Disclosure Bull.* **24,** 1922 (1981).

31. A. C. Tam, "Localized Persistent Polarization in Layered Organic Photoconductors," *IBM Tech. Disclosure Bull.* **24,** 2393 (1981).
32. C. F. Carlson, "Electrophotographic Apparatus," U.S. Patent 2,357,809, 1944.
33. For a discussion of Se and its alloys, see P. H. Keck, "Photosensitive Selenium Plates," U.S. Patent 2,739,079, March 20, 1956.
34. S. Tanaka, "Electrophotographic Process Using a Cadmium Sulfide Photoconductor having Hysteresis Character—Variation of the Amount of Light during Exposure to Improve Image Formation," U.S. Patent 4,142,889, March 6, 1979.
35. H. W. Anderson and M. T. Moore, "Hydrozone Containing Charge Transport Element and Photoconductive Process of Using Same—Electrography," U.S. Patent 4,150,987, March 24, 1977.
36. W. J. Dulmage, W. A. Light, S. J. Marino, C. D. Salzberg, D. L. Smith, and W. J. Standenmayer, "An Aggregate Organic Photoconductor. I. Chemical Composition, Preparation, Physical Structure, and Optical Properties," *J. Appl. Phys.* **49,** 5543–5554 (1978).
37. Evan S. Baltazzi, "Recent Developments in Electrophotographic Processes, Materials, and Related Fields," *J. Appl. Photog. Eng.* **6,** 147–152 (1980).
38. An example of such a machine configuration can be found in the IBM 6670 intelligent copier.
39. J. M. Fleischer, M. R. Latta, and M. E. Rabedeau, "Laser-Optical System of the IBM 3800 Printer," *IBM J. Res. Develop.* **21,** 479–483 (1977).
40. U. Vahtra and R. F. Wolter, "Electrophotographic Process in a High Speed Printer," *IBM J. Res. Develop.* **22,** 34–39 (1978).
41. J. J. Coleman, N. Holonyak, Jr., M. J. Ludowise, and P. D. Wright, "Yellow $In_{1-x}Ga_xP_{1-z}As_z$ Double Heterojunction Lasers," *J. Appl. Phys.* **47,** 2015–2019 (1976).
42. Canon, Inc., Tokyo, Model LBP-10 Laser Printer, announced in 1979.
43. G. N. Schrauzer and V. P. Mayweg, "Reaction of Diphenylacetylene with Nickel Sulfides," *J. Amer. Chem. Soc.* **84,** 3221 (1962).
44. *Color Index,* Third Edition, The Society of Dyers and Colorists, New York, 1971.

Received March 17, 1981; revised September 21, 1981

Andrew C. Tam is located at the IBM Research Division laboratory, 5600 Cottle Road, San Jose, California 95193. Richard D. Balanson is with the IBM Corporate Headquarters Division at Old Orchard Road, Armonk, New York 10504.